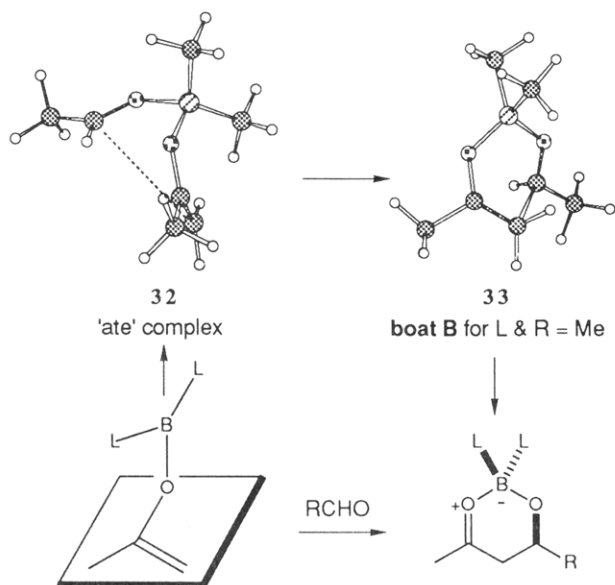


Scheme VI



### Conclusions

The force field developed enables the prediction of preferred enol borinate geometries in synthetically useful chiral systems. The preferred geometry is calculated to be nonplanar in all cases, and we look forward to an experimental test of this prediction. The preferred geometry appears to be decided by a large number of competing effects, rather than one or two factors, and so cannot be easily considered by model building, nor by a simple di-

vision of the substituents at the chiral centers into large, medium, and small groups. Studies of these systems using the force field suggest that the sense of  $\pi$ -face stereoselectivity may be predicted from the preferred enol borinate conformation using a Zimmerman-Traxler argument for *Z*-methyl enol borinates, with isopinocampheyl ligands as the chiral directing groups. If the chiral directing group is in the ketone, the enol borinate geometry does not appear to be directly related to the observed aldol product stereochemistry. Here the structure of the "ate" complex and the aldol transition state must be important and we are now considering these in more detail.

The calculations have suggested a possible explanation for the surprising reverse in the sense of aldehyde enantioface selectivity between methyl and ethyl ketones using enol diisopinocampheyl borinates. The reversed sense of the stereoselectivity may be due to competing transition states and not to different enolate  $\pi$ -face selectivity.

**Acknowledgment.** We thank the SERC and Lilly Research Centre (CASE Award to J.M.G.), Churchill College (Fellow Commonership to S.D.K.), the Cambridge Computing Service, Gonville and Caius College, Merck Sharpe and Dohme, and the Donors of the Petroleum Research Fund, administered by the American Chemical Society, for support. We thank Dr. W. J. Ross (Lilly) for his continued interest in this work and Professor C. Genari (Milan) for helpful discussions assisted by a NATO grant (0369/88).

**Supplementary Material Available:** A listing of all enol borinate structures discussed (31 pages). Ordering information is given on any current masthead page.

## On the Regioselectivity of 4-Nitroanisole Photosubstitution with Primary Amines. A Mechanistic and Theoretical Study

Albert Cantos, Jorge Marquet,\* Marcial Moreno-Mañas, Angels González-Lafont, José M. Lluch,\* and Juan Bertrán

Department of Chemistry, Universitat Autònoma de Barcelona, 08193 Bellaterra, Barcelona, Spain

Received July 3, 1989

4-Nitroanisole photoreacts with *n*-hexylamine and ethyl glycinate, giving rise to regioselective methoxy and nitro group photosubstitution, respectively. Mechanistic evidence indicates that the latter is produced through a  $S_N2^3Ar^*$  reaction, whereas the former arises from a radical ion pair via electron transfer from the amine to a 4-nitroanisole triplet excited state. AM1 semiempirical calculations on the actually involved excited states and intermediates indicate that the change of regioselectivity between the ground-state and the triplet-state substitution can be justified on the basis of frontier orbital considerations. On the other hand, neither the frontier orbital nor the net charge can explain the regioselectivity when the reaction involves electron transfer. A discussion of the influence of other previously neglected factors such as the intermediate stabilities is advanced.

### Introduction

Nucleophilic aromatic photosubstitutions have been the object of intense research since their discovery in 1956.<sup>1</sup> In spite of the effort, mechanistic studies have been for years restricted almost to photohydrolysis reactions.<sup>2-4</sup>

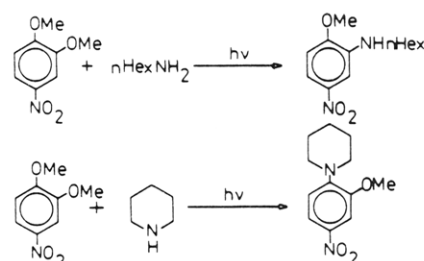
(1) (a) Cornelisse, J.; Havinga, E. *Chem. Rev.* **1975**, *75*, 353. (b) Havinga, E.; Cornelisse, J. *Pure Appl. Chem.* **1976**, *47*, 1. (c) Cornelisse, J.; Lodder, G.; Havinga, E. *Rev. Chem. Intermed.* **1979**, *2*, 231.

(2) Cornelisse, J.; De Gunst, G. P.; Havinga, E.; *Adv. Phys. Org. Chem.* **1975**, *11*, 225.

(3) Varma, C. A. G. O.; Tamminga, J. J.; Cornelisse, J. *J. Chem. Soc., Faraday Trans. 2* **1982**, *78*, 225.

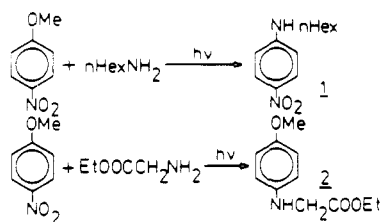
(4) Van Zeijl, P. H. M.; van Eijk, L. M. J.; Varma, C. A. G. O. *J. Photochem.* **1985**, *29*, 415.

Scheme I



Many reported experimental facts remain unexplained, especially in cases when nucleophiles others than  $OH^-$  are used.

Scheme II



Van Riel et al.<sup>5</sup> have pointed out the existence of three kinds of pathways leading to nucleophilic aromatic photosubstitutions: (1) direct displacement ( $S_N2Ar^*$ ); (2) electron transfer from the "nucleophile" to the aromatic substrate; and (3) electron transfer from the aromatic compound to an acceptor followed by attack of the nucleophile on the aromatic radical cation. In recent years several research groups have directed their attention to these reactions.<sup>3-12</sup> In the course of our investigation of the photosubstitution of 4-nitroveratrole with amines (Scheme I), we found<sup>13</sup> that the regioselectivity of these reactions depends on the ionization potential of the nucleophile. A mechanistic borderline between  $S_N2Ar^*$  reactions (for high ionization potential amines) and electron transfer from the amine to the substrate triplet excited state (for low ionization potential amines) was proposed on the basis of continuous irradiation<sup>14,15</sup> and laser flash photolysis<sup>16</sup> experiments. Some other related regioselectivity changes have been reported for photo-Smiles reactions<sup>6,7</sup> and for the photosubstitution of 1-methoxy-1-nitronaphthalene with nucleophiles.<sup>12</sup>

The nitroanisoles, particularly *m*- and *p*-nitroanisoles, are probably the most thoroughly investigated compounds in nucleophilic aromatic photosubstitution reactions.<sup>1</sup> 4-Nitroanisole photoreacts<sup>17</sup> readily with amines in aqueous solution, giving rise to methoxy group substitution. Nevertheless, Letsinger<sup>18</sup> reported the formation of 1-(4-methoxyphenyl)pyridinium nitrite in the photoreaction between 4-nitroanisole and pyridine.

We have found an even more striking example of regioselectivity change in the photoreactions shown in Scheme II. Thus, some years ago we reported<sup>13</sup> that ethyl glycinate (GlyNH<sub>2</sub>) photosubstitutes the nitro group in 4-nitroanisole in spite of being a primary amine. We wish to describe here a continuous irradiation-based mechanistic

study showing that this regioselectivity change constitutes another example of a change in the mechanistic pathway. True  $S_N2Ar^*$  reactions in 4-nitroanisole lead to nitro-group photosubstitution, whereas the observed methoxy-group photosubstitution when amines other than GlyNH<sub>2</sub> are used must be attributed to an alternative mechanistic path that includes electron transfer from the amine to a triplet excited state of the substrate. The outcome of the reaction depends on the ionization potential of the used nucleophile. Our results show that the regioselectivity changes described in Schemes I and II are consequences of the same mechanistic phenomenon.

Based on their studies on photo-Smiles rearrangement reactions,<sup>6,7</sup> and partially using a hypothesis advanced by Epiotis,<sup>19</sup> Mutai et al.<sup>20,21</sup> have recently suggested that in several systems the course of nucleophilic photosubstitution could be predicted from an examination of the frontier molecular orbitals of the aromatic substrate. They view  $S_N2Ar^*$  reactions as involving principally an interaction between the nucleophile HOMO and an orbital that would correlate with the aromatic substrate's ground-state HOMO; the nucleophile attacks the position(s) where the MO coefficient of the aromatic substrate's HOMO is higher. An alternative interaction is between the LUMO of the aromatic substrate and the HOMO of the nucleophile; if an electron is transferred from the "nucleophile" to the aromatic substrate, the nucleophile radical cation will then attack at the position where the aromatic substrate has the highest LUMO coefficient. We believe this approach is too simple, since upon electronic excitation and electron transfer, energies, coefficients, and charges of the involved orbitals of the substrate excited state and radical anion will be very different from those in the ground state. It is also hard to believe that a reaction between two charged species like a radical anion and a radical cation is going to be mainly frontier orbital controlled without any charge contribution. Therefore, we will also describe here a series of theoretical calculations carried out using the AM1 semiempirical method (previously shown by us reasonably appropriate to describe excited states<sup>22</sup>) on the excited states and radical ions of 4-nitrophenol (as a model of 4-nitroanisole). Consideration of the real involved spin orbitals give some support to Mutai's interpretation only for photoreactions where neutral excited states are involved ( $S_N2Ar^*$ ). A new reasoning, perhaps including other previously ignored factors such as  $\sigma$ -complex stabilities, is needed to justify the photosubstitution regioselectivity in cases where radical-ion collapse is a key step.

### Preparative and Kinetic Results

The preparative photoreaction between 4-nitroanisole and excess *n*-hexylamine in MeOH-water (20:80 v/v) (2 h irradiation with a 400-W medium-pressure Hg lamp and Pyrex filter) gave *N*-(1-hexyl)-4-nitroaniline (1) as the only photosubstitution product (16% yield based on the consumed starting material) (Scheme II). Product 1 was fully characterized by spectroscopic methods and by comparison with a sample independently prepared by thermal substitution reaction.

The preparative photoreaction between excess ethyl glycinate and 4-nitroanisole was carried out in a similar

(5) Van Riel, H. C. H. A.; Lodder, G.; Havinga, E. *J. Am. Chem. Soc.* **1981**, *103*, 7257.

(6) Mutai, K.; Yokoyama, K.; Kanno, S.; Kobayashi, K. *Bull. Chem. Soc. Jpn.* **1982**, *55*, 1112.

(7) Mutai, K.; Kobayashi, K.; Yokoyama, K. *Tetrahedron* **1984**, *40*, 1755.

(8) Wubbels, G. G. *Acc. Chem. Res.* **1983**, *16*, 285.

(9) Wubbels, G. G.; Susens, D. P.; Coughlin, E. B. *J. Am. Chem. Soc.* **1988**, *110*, 2538.

(10) Wubbels, G. G.; Snyder, E. J.; Coughlin, E. B. *J. Am. Chem. Soc.* **1988**, *110*, 2543.

(11) Wubbels, G. G.; Severson, B. R.; Sanders, H. *J. Am. Chem. Soc.* **1989**, *111*, 1018.

(12) Bunce, N. J.; Cater, S. R.; Scaiano, J. C.; Johnston, L. J. *J. Org. Chem.* **1987**, *52*, 4214.

(13) Cervelló, J.; Figueredo, M.; Marquet, J.; Moreno-Mañas, M.; Bertrán, J.; Lluch, J. M. *Tetrahedron Lett.* **1984**, *25*, 4147.

(14) Cantos, A.; Marquet, J.; Moreno-Mañas, M. *Tetrahedron Lett.* **1987**, *28*, 4191.

(15) Cantos, A.; Marquet, J.; Moreno-Mañas, M.; Castelló, A. *Tetrahedron* **1988**, *44*, 2607.

(16) Van Eijk, A. M. J.; Huizer, A. H.; Varma, C. A. G. O.; Marquet, J. *J. Am. Chem. Soc.* **1989**, *111*, 88.

(17) Kronenberg, M. E.; van der Heyden, A.; Havinga, E. *Recl. Trav. Chim. Pays-Bas* **1966**, *85*, 56.

(18) Letsinger, R. L.; Ramsey, O. B.; McCain, J. H. *J. Am. Chem. Soc.* **1965**, *87*, 2945.

(19) (a) Epiotis, N. D. *Theory of Organic Reactions*; Springer-Verlag: New York, 1978. (b) Epiotis, N. D.; Shaik, S. J. *J. Am. Chem. Soc.* **1978**, *100*, 29.

(20) Mutai, K.; Nakagaki, R.; Takeda, H. *Bull. Chem. Soc. Jpn.* **1985**, *58*, 2066.

(21) Mutai, K.; Nakagaki, R. *Bull. Chem. Soc. Jpn.* **1985**, *58*, 3663.

(22) González-Lafont, A.; Lluch, J. M.; Bertrán, J.; Marquet, J. *Spectrochim. Acta* **1988**, *44A*, 1427.

**Table I. Effect of Triplet Quenchers, Radical Scavengers, and Solvents on the Photoreactions of 4-Nitroanisole with *n*-Hexylamine and Ethyl Glycinate<sup>a</sup>**

expt	amine	blank <sup>b</sup>	solvent and irradiation time (min)	additives	product	$\phi/\phi_{\text{blank}}^c$
1	<i>n</i> -C <sub>6</sub> H <sub>13</sub> NH <sub>2</sub>	<i>d</i>	MeOH/H <sub>2</sub> O (20:80), 15	potassium sorbate <sup>e</sup>	1	0.27
2	H <sub>2</sub> NCH <sub>2</sub> CO <sub>2</sub> Et	<i>d</i>	MeOH/H <sub>2</sub> O (20:80), 30	potassium sorbate <sup>f</sup>	2	0.48
3	<i>n</i> -C <sub>6</sub> H <sub>13</sub> NH <sub>2</sub>	<i>d</i>	MeOH/H <sub>2</sub> O (20:80), 15	<i>m</i> -dinitrobenzene <sup>g</sup>	1	0.05
4	H <sub>2</sub> NCH <sub>2</sub> CO <sub>2</sub> Et	<i>d</i>	MeOH/H <sub>2</sub> O (20:80), 15	<i>m</i> -dinitrobenzene <sup>g</sup>	2	0.82
5	<i>n</i> -C <sub>6</sub> H <sub>13</sub> NH <sub>2</sub>	<i>h</i>	MeOH/H <sub>2</sub> O (20:80), 3	MV <sup>2+</sup> 2Cl <sup>-i</sup>	1	0.01
6	H <sub>2</sub> NCH <sub>2</sub> CO <sub>2</sub> Et	<i>h</i>	MeOH/H <sub>2</sub> O (20:80), 3	MV <sup>2+</sup> 2Cl <sup>-i</sup>	2	1
7	<i>n</i> -C <sub>6</sub> H <sub>13</sub> NH <sub>2</sub>	<i>j</i>	MeOH, 30		1	0
8	H <sub>2</sub> NCH <sub>2</sub> CO <sub>2</sub> Et	<i>j</i>	MeOH, 30		2	0.02

<sup>a</sup>The present data have been previously reported in ref 22 (125-W Hg high-pressure lamp). <sup>b</sup>Each reaction was carried out in parallel to a blank (using a standard solvent mixture, MeOH/H<sub>2</sub>O 20/80, and in the absence of additives). No precautions were taken to avoid oxygen, except for expt 5 and 6. <sup>c</sup>Ratio between the chromatographic peak areas corresponding to the studied photoproduct, referred to the chromatographic peak area of a fixed amount of internal reference in each case, and the same in the blank experiment. <sup>d</sup>4-Nitroanisole (1.9 × 10<sup>-2</sup> M), amine (0.47 M). <sup>e</sup>0.1 M. <sup>f</sup>0.22 M. <sup>g</sup>0.07 M. <sup>h</sup>4-Nitroanisole (5.6 × 10<sup>-3</sup> M), amine (1.7 × 10<sup>-2</sup> M). <sup>i</sup>Methyl viologen (6.55 × 10<sup>-4</sup> M). <sup>j</sup>4-Nitroanisole (6.5 × 10<sup>-3</sup> M), amine (4.6 × 10<sup>-3</sup> M).

**Table II. Overall Quantum Yield of Production of 1 in the Photoreaction of 4-Nitroanisole (1.5 × 10<sup>-3</sup> M) with *n*-Hexylamine (Nu) in Methanol/Water (20:80 v/v) at Different Nucleophile Concentrations**

[Nu] <sup>a</sup>	0.094	0.241	0.290	0.388	0.487	0.585
$\phi^{366} \times 10^3$	9.5	14.7	17.3	17.0	17.6	17.6

<sup>a</sup>Amine real concentrations once the amount of ammonium cation produced by hydrolysis is subtracted.

way. The ethyl glycinate was used in the hydrochloride form and liberated in situ by using the stoichiometric amount of sodium hydroxide. The irradiation was kept for 13 h and *N*-ethoxycarbonylmethyl-4-methoxyaniline (2) was obtained in 15% isolated yield as the only photosubstitution product.

**Qualitative Experiments.** In Table I, the effects of triplet quenchers, radical scavengers, and solvent polarity on the photoreactions of Scheme II are described. Those experiments have been previously reported without experimental detail and discussed in a preliminary note.<sup>23</sup> Experiments 1 and 2 suggest the involvement of triplet excited states in the photoreaction paths. Quantitative studies (vide infra) have confirmed this conclusion. Parallel reactions carried out in the presence and in the absence of *m*-dinitrobenzene showed a much more important decrease in photosubstitution efficiency, when the radical scavenger was present, in the case of *n*-hexylamine (expt 3) than in the case of ethyl glycinate (expt 4). The same happened (expt 5 and 6) using methyl viologen (strong electron acceptor and radical scavenger). In addition only expt 5 showed the strong blue color attributed to the methyl viologen cation ( $\lambda_{\text{max}} = 600 \text{ nm}$ ).<sup>24</sup> We interpret these results considering that methoxy group photosubstitution produced by *n*-hexylamine is the result of a single electron transfer from the amine to the 4-nitroanisole excited triplet state. On the other hand, electron transfer does not seem to play a significant role in the photoreaction affording the *N*-ethoxycarbonylmethyl-4-methoxyaniline, and it is therefore reasonable to assign this reaction to a S<sub>N</sub>2<sup>3</sup>Ar\* mechanism.

The effect of solvent change (expt 7 and 8) can be rationalized by considering the decrease of excited-state stabilization through the hydrogen bond<sup>25</sup> on going from water to methanol. This would reduce the triplet excited-state lifetime, decreasing the photoreaction efficiency.

**Quantum Yield Measurements.** We decided to carry out quantitative measurements in order to support the previously proposed mechanistic scheme<sup>22</sup> and to get some insight for the kinetic scheme of the studied reactions (Scheme II).

Overall quantum yields for the production of 1 and 2 were measured at different nucleophile concentrations (Tables II and III). Quantum yields increase by increasing the nucleophile concentration in both cases. The multiplicity of the reactive excited states was investigated using potassium sorbate as selective triplet quencher (Tables IV and V). There is a significant quenching effect due to potassium sorbate in both cases which indicates the involvement of triplet excited states in both photoreactions of Scheme II.

### Kinetic Discussion

On the basis of the above results and others previously reported by us in related systems,<sup>14-16</sup> we suggest the overall kinetic scheme of Scheme III for the reactions considered in the present work.

The species Y can be assigned to an ensemble of  $\sigma$ -complexes (Meisenheimer type), possibly in the ground-state surface, in the photoreaction with ethyl glycinate as nucleophile. On the other hand, Y will correspond to a radical-ion pair that will collapse into the  $\sigma$ -complexes in a further step, in the photoreaction carried out with *n*-hexylamine as nucleophile. Some of the  $\sigma$ -complexes will evolve to a final photosubstitution product by losing a good leaving group (NO<sub>2</sub>, methoxy, in our case), the others reverting to the original ground state.

The application of the steady-state approximation in Scheme III in the absence of quencher leads to the equation:

$$\phi = \phi_{\text{isc}} \frac{k_p}{k_p + k_d} \frac{k_3[\text{Nu}]}{k_2 + k_3[\text{Nu}]} \quad (1)$$

and from eq 1

$$\frac{1}{\phi} = \frac{1}{\phi_{\text{isc}}} \frac{k_p + k_d}{k_p} \left( 1 + \frac{k_2}{k_3[\text{Nu}]} \right) \quad (2)$$

Therefore, if the scheme applies and the photosubstitution products come from a unique origin, a linear relationship between  $\phi^{-1}$  and  $[\text{Nu}]^{-1}$  should be observed. Indeed this is the case, and the representations for the studied photoreactions (Scheme II) are shown in Figure 1. A regression analysis of the dependence of  $\phi^{-1}$  upon  $[\text{n-C}_6\text{H}_{13}\text{NH}_2]^{-1}$  (Figure 1A) using the values of Table II gave a linear equation (correlation coefficient (c.c.) 0.988):

$$\phi^{-1} = (43.9 \pm 2.2) + (5.7 \pm 0.4)[\text{n-C}_6\text{H}_{13}\text{NH}_2]^{-1}$$

(23) Cantos, A.; Marquet, J.; Moreno-Mañas, M. *Tetrahedron Lett.* 1989, 30, 2423.

(24) Duonghong, D.; Borgarello, E.; Grätzel, M. *J. Am. Chem. Soc.* 1981, 103, 4685.

(25) Varma, C. A. G. O.; Plantenga, F. L.; Huizer, A. H.; Zwart, J. P.; Bergwerf, Ph.; Van der Ploeg, J. P. M. *J. Photochem.* 1984, 24, 133.

**Table III. Overall Quantum Yields of Production of 2 in the Photoreaction of 4-Nitroanisole ( $1.5 \times 10^{-3}$  M) with Ethyl Glycinate (Nu) in Methanol/Water (20:80 v/v) at Different Nucleophile Concentrations**

[Nu] <sup>a</sup> $\phi^{366} \times 10^3$	0.023	0.046	0.090	0.14	0.18	0.27	0.36	0.50	0.80	1.00
	2.9	4.2	5.4	6.4	6.7	6.9	7.3	7.4	7.5	7.7

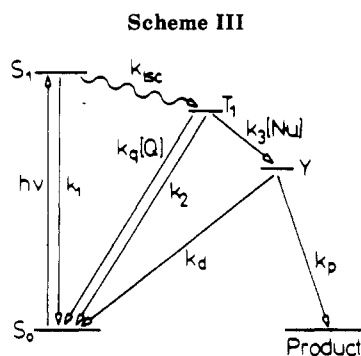
<sup>a</sup> Amine real concentrations once the amount of ammonium cation produced by hydrolysis is subtracted.

**Table IV. Overall Quantum Yields of Production of 1 in the Photoreaction of 4-Nitroanisole ( $1.5 \times 10^{-3}$  M) with *n*-Hexylamine (0.487 M) in Methanol/Water (20:80 v/v) in the Presence of Different Concentrations of Potassium Sorbate (Q)**

[Q] $\phi^{366} \times 10^3$	0	0.028	0.122	0.195	0.269	0.360	0.412
	17.6	16.6	12.7	10.3	9.2	8.0	7.3

**Table V. Overall Quantum Yields of Production of 2 in Photoreactions of 4-Nitroanisole ( $1.5 \times 10^{-3}$  M) with Ethyl Glycinate (0.499 M) in Methanol/Water (20:80 v/v) in the Presence of Different Concentrations of Potassium Sorbate (Q)**

[Q] $\phi^{366} \times 10^3$	0	0.04	0.09	0.13	0.18
	7.4	6.5	4.4	3.5	2.6



From eq 2 we have  $k_2/k_3$  equal to the slope to intercept ratio; therefore,  $k_2/k_3 = 0.13$  for *n*-hexylamine. A similar analysis for the photoreaction of ethyl glycinate (EtGly) using the values of Table III leads to a linear equation (c.c. 0.999):

$$\phi^{-1} = (124.4 \pm 1.3) + (5.19 \pm 0.08)[\text{EtGly}]^{-1}$$

and from this  $k_2/k_3 = 0.042$ . The inverse relationship  $k_3/k_2$  indicates the efficiency of the productive interaction between the nucleophile and the excited state being larger for ethyl glycinate but of similar magnitude.

According to the Stern-Volmer analysis, the dependence of the relative reciprocal quantum yield on the quencher concentration is given by:

$$\frac{\phi_0}{\phi} = 1 + \frac{k_q[Q]}{k_3[\text{Nu}] + k_2} \quad (3)$$

The plot of  $\phi_0/\phi$  vs [Q] in the considered processes (Figure 2) and the corresponding regression analyses using the data of Tables IV and V lead to straight lines in both cases. Thus for *n*-hexylamine (c.c. 0.988):

$$\phi_0/\phi = (0.99 \pm 0.02) + (3.44 \pm 0.08)[Q]$$

and for ethyl glycinate (0.984):

$$\phi_0 = (0.84 \pm 0.12) + (10.4 \pm 1.1)[Q]$$

These results confirm the triplet excited state as intermediate. The analysis of the values obtained from the straight lines in Figure 2 leads to interesting conclusions. Thus,  $k_q/(k_2 + k_3[\text{Nu}]) = 3.4$  for *n*-hexylamine and 10.4 for ethyl glycinate.

The triplet energy of 4-nitroanisole is known<sup>26</sup> to be  $E_T$

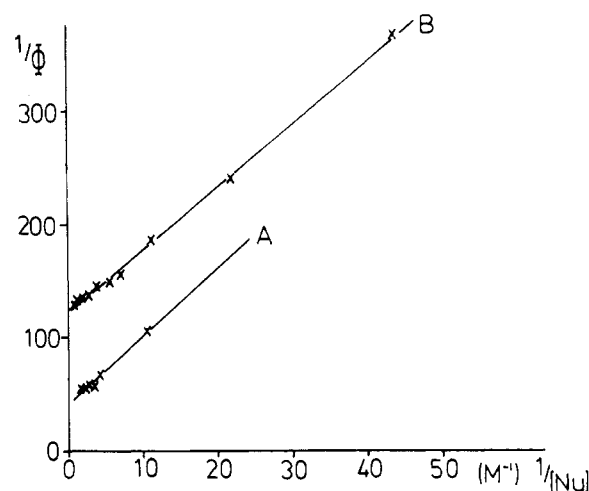


**Figure 1.** Plot of inverse quantum yield of production of photosubstitution product vs inverse nucleophile concentrations: (A) photosubstitution of 4-nitroanisole with *n*-hexylamine (OMe substitution, 1, data from Table II); (B) photosubstitution of 4-nitroanisole with ethyl glycinate (NO<sub>2</sub> substitution, 2, data from Table III).

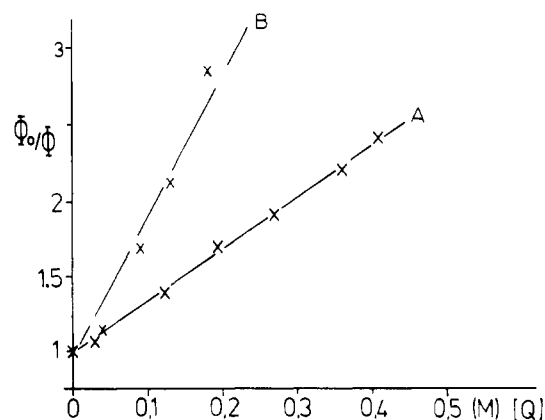


**Figure 2.** Plot of the relative inverse quantum yield of 4-nitroanisole photosubstitution vs quencher concentrations (potassium sorbate): (A) *n*-hexylamine nucleophile, (B) ethyl glycinate nucleophile.

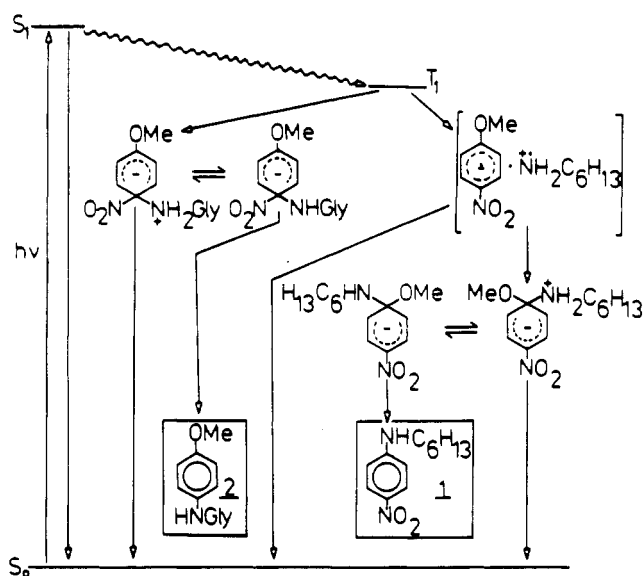
= 60 kcal/mol. This value has been obtained from phosphorescence measurements at 77 K in hydrocarbon solvents. A general feature when the known<sup>4,9</sup>  $k_q$ 's (energy-transfer mechanism) of nitromethoxybenzenes in aqueous solvents are considered is the fact that their values are in many cases lower by as much as one order of magnitude than the corresponding diffusion-controlled limit. Varma<sup>4</sup> has suggested that the stabilization of the triplet excited state by hydrogen bonding in water can justify the low  $k_q$  values observed in many cases. This explanation

would also justify the observed increase of  $k_q$  value with decreasing concentration of water in several examples. Considering the previous reasoning and the rate constant diffusion-controlled limit in our conditions ( $k_{diff} = 9 \times 10^9 \text{ M}^{-1} \text{ s}^{-1}$  at  $30^\circ \text{C}$  calculated by the Debye equation<sup>27</sup>), and in order to make comparisons, we approximate  $k_q \approx 10^9 \text{ M}^{-1} \text{ s}^{-1}$  in our case. Using this value  $k_3 \approx 5 \times 10^8 \text{ M}^{-1} \text{ s}^{-1}$  for *n*-hexylamine and  $k_3 \approx 2 \times 10^8 \text{ M}^{-1} \text{ s}^{-1}$  for ethyl glycinate. These results indicate  $k_{3(n\text{-hexylamine})} > k_{3(\text{EtGly})}$  being both of the same order. This means that the previously commented higher efficiency for the productive interaction between the amine and the triplet excited state for ethyl glycinate is due to a lower value of the triplet decay constant  $k_2$  ( $k_{2(n\text{-hexylamine})} \approx 6 \times 10^7 \text{ s}^{-1}$  vs  $k_{2(\text{EtGly})} \approx 7 \times 10^6 \text{ s}^{-1}$ ). This significant difference can be justified considering  $k_2$  represents several photophysical and photochemical possible processes, among them (i) radiative decay; (ii) nonradiative decay; (iii) nucleophile-induced quenching, which would include quenching induced by the amine and quenching induced by the  $\text{OH}^-$  generated in the hydrolysis of the amine [the higher basicity of *n*-hexylamine ( $k_{b(n\text{-hexylamine})} = 3.63 \times 10^{-4}$  and  $k_{b(\text{EtGly})} = 5.62 \times 10^{-7}$ ) will produce the presence of a higher concentration of  $\text{OH}^-$  ion in the photoreactions using that nucleophile]; and, finally, (iv) photohydrolysis resulting from the productive interaction of the triplet excited state with  $\text{OH}^-$  generated in the hydrolysis of the nucleophile. Points iii and iv require a dependence of  $k_2$  on the amine and  $\text{OH}^-$  concentrations. Nevertheless, the reasonably good fits obtained (Figure 1) indicate that  $k_2$  can be considered constant in the relatively narrow range of nucleophile concentrations used. Those fits also allow us to neglect (in our range of nucleophile concentrations) the predictable existence of general base catalysis<sup>8</sup> in our photoreactions.

Our results (Tables II and III, and Figure 1) show that  $k_p$  competes poorly with  $k_d$  in both studied cases. This seems reasonable for the *n*-hexylamine case since  $k_d$  includes decay (and any other process not leading to photosubstitution), both from the radical-ion pair and the  $\sigma$ -complexes (Schemes III and IV). Collapse of the radical-ion pair involves intersystem crossing, and the competing diffusion away of the pair must be much more important in our intermolecular photoreactions than in related intramolecular cases described in the literature.<sup>6-8</sup> On the other hand, the low efficiency shown in this step by the ethyl glycinate photoreaction is surprising considering related cases described in the literature, even for intermolecular photoreactions,<sup>15</sup> and the relative large amount of bases around that would catalyze the process by deprotonating the zwitterionic  $\sigma$ -complex (Scheme IV). We attribute this poor efficiency to the lower ability of the  $\text{NO}_2$  group with respect to  $\text{RO}^-$  as leaving group. Even though the nitrite is generally considered to be a good leaving group in nucleophile aromatic substitution, this seems<sup>28</sup> to be due to the fact that those thermal reactions occur in two steps, the first (attack of the nucleophile to the aromatic ring) being the rate-determining step. This step is favored by strong electron-attracting groups such as  $\text{NO}_2$ . In our case the  $\sigma$ -complex is already formed, the efficiency of the last step depending upon the intrinsic leaving-group ability of  $\text{NO}_2^-$ , that, as our results suggest, must be rather poor compared to that of  $\text{RO}^-$ .

On the basis of all the preparative, qualitative, and quantitative commented results, and taking into consideration related cases reported in the literature,<sup>12,15,16</sup> we propose the overall mechanistic scheme depicted in

Scheme IV



Scheme IV for the photoreactions of 4-nitroanisole with amine nucleophiles. It is remarkable that the previously reported similar borderlines for mechanistic changes (4-nitroveratrole<sup>15</sup> and 1-methoxy-4-nitronaphthalene<sup>12</sup>), placed between primary and secondary amines, are shifted for 4-nitroanisole to higher values of ionization potential (different primary amines), in agreement with the larger electronic affinity of this system. A clear mechanistic picture is now emerging for the photoreactions of nitrophenyl ethers with nucleophiles.

### Theoretical Calculations and Discussion

With the aim of discussing theoretically the main factors that control the regioselectivity of the nucleophilic aromatic photosubstitutions, we have chosen, as a good example of regioselectivity change, the reactions of 4-nitroanisole with *n*-hexylamine and ethyl glycinate just mechanistically discussed. For the sake of simplicity we have replaced the methoxy group by hydroxy, the 4-nitrophenol being the actually calculated structure. In addition, methyl glycinate instead of ethyl glycinate has been used.

All the molecular orbital (MO) calculations presented in this work were carried out using the semiempirical AM1 method,<sup>29,30</sup> implemented in the AMPAC<sup>31</sup> program. To take into account the previously commented different mechanistic paths, several electronic states (the ground singlet state ( $S_0$ ), the first excited singlet state ( $S_1$ ), and the lowest triplet state ( $T_1$ )) of 4-nitrophenol and its radical anion (RA) have been considered. Moreover, the ground singlet states and the corresponding radical cations of *n*-hexylamine and methyl glycinate have been also calculated. The ground-state geometries were completely optimized, the energy being calculated at the restricted Hartree-Fock (RHF)<sup>32</sup> level. The geometries obtained in this way have been kept invariant to compute the radicals and the excited states arising from each ground state. The half-electron method<sup>33</sup> was adopted to determine the

(29) Dewar, M. J. S.; Storch, D. M. *J. Am. Chem. Soc.* **1985**, *107*, 3898.

(30) Dewar, M. J. S.; Zoebisch, E. G.; Healy, E. F.; Stewart, J. J. P. *J. Am. Chem. Soc.* **1985**, *107*, 3902.

(31) Stewart, J. J. P. *QCPE Bull.* **1986**, *6*, 24.

(32) Roothaan, C. C. J. *Rev. Mod. Phys.* **1951**, *23*, 69.

(33) Dewar, M. J. S.; Hashmall, J. A.; Venier, C. G. *J. Am. Chem. Soc.* **1968**, *90*, 1953.

(27) Debye, P. J. *Trans. Electrochem. Soc.* **1942**, *82*, 265.

(28) Beck, J. R. *Tetrahedron* **1978**, *34*, 2057.

Table VI. Numerical Values of the Energy Levels (in eV) Corresponding to the Orbitals Depicted in the Figure 3

	4-nitrophenol						<i>n</i> -hexylamine			methyl glycinate		
	S <sub>0</sub>	S <sub>1</sub>	T <sub>1</sub>		RA		G	RC		G	RC	
			α	β	α	β		α	β			
nL	-0.42	-0.26	-0.28	0.39	4.91	5.02	2.87	-3.74	-3.92	1.85	-4.09	-4.22
L	-1.07	-3.72	-8.03	-0.35	-2.06	4.94	1.60	-5.56	-6.26	0.98	-4.16	-4.55
H	-10.07	-7.41	-11.05	-3.0	-5.48	-4.67	-8.43	-7.14	-14.13	-10.33	-9.07	-15.83
nH	-10.76	-11.00	-11.7	-10.96	-5.98	-5.81	-11.03	-14.13	-14.59	-11.63	-15.82	-16.43

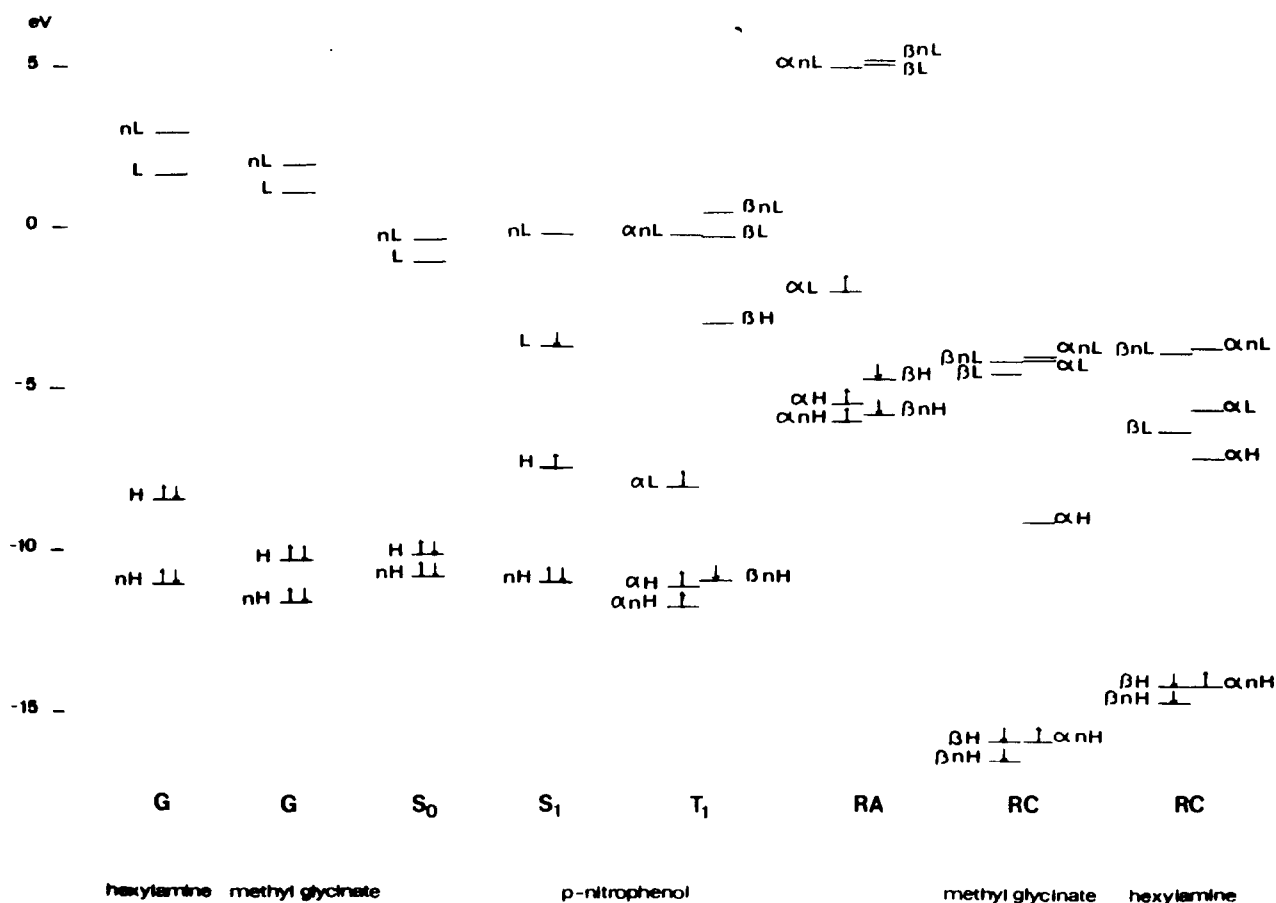


Figure 3. Energy levels of the frontier and some near-to-frontier orbitals for the different considered species of ethyl glycinate, *n*-hexylamine, and 4-nitrophenol: G, ground state of the amines; S<sub>0</sub>, S<sub>1</sub>, T<sub>1</sub>, ground, singlet, and triplet excited states of 4-nitrophenol, respectively; RA, radical anion of 4-nitrophenol; RC, radical cations of the amines.

molecular orbitals of the S<sub>1</sub> state. This method replaces the electron in a singly occupied MO by two "half-electrons" with opposite spin. In this way S<sub>1</sub> can be handled by the standard closed-shell procedure. In dealing with systems wherein the number of α electrons is different from the number of β electrons, we have preferred the unrestricted Hartree-Fock (UHF)<sup>34</sup> method that allows for spin polarization. Using this procedure, the components with the values  $M_s = 1$  of the triplet state,  $M_s = 1/2$  of the radical anion, and  $M_s = -1/2$  of the radical cations were calculated.

In Figure 3 (Table VI), the energy levels of the frontier and some near-to-frontier orbitals for the different calculated species are depicted. It should be emphasized that each restricted molecular orbital of the ground or the S<sub>1</sub> states can accommodate a pair of electrons, whereas each unrestricted molecular spin orbital of the triplet or the radicals can bear only one electron. As expected, two different sets of unrestricted α-spin orbitals and β-spin orbitals are obtained, due to the spin polarization. For the ground states the symbols nH, H, L, and nL stand for the

classical next-HOMO, HOMO, LUMO, and next-LUMO, respectively. For the remaining species the same nomenclature has been maintained with the aim of indicating just how each orbital correlates with the well-defined ground-state orbitals. In spite of this correlation it must be recalled that the MO coefficients vary from one species to another.

From a first inspection of Figure 3 (Table VI), several features merit mention. First, on going from S<sub>0</sub> to S<sub>1</sub> the H orbital of S<sub>0</sub> loses one electron, its energy being raised. Conversely, the L orbital of S<sub>0</sub> gains one electron, its energy being lowered. Second, when the UHF method is used, the occupied spin orbitals appear clearly below their corresponding empty spin-orbital partners. Third, in the T<sub>1</sub> state and the RA system, the excess of α electrons pushes down the α-spin orbitals relative to the β-spin orbitals because of exchange interactions that are present only between electrons of the same spin. Fourth, in the radical anion all the orbitals undergo an important raising due to the interelectronic repulsion resulting from the presence of an extra electron. Finally, regarding the amines, the occupied orbitals of *n*-hexylamine lie above the corresponding ones of methyl glycinate. That means the former amine is a softer nucleophile, its ionization potential being

(34) Pople, J. A.; Nesbet, R. K. *J. Chem. Phys.* 1954, 22, 571.

lower. When the radical cations are formed, all the orbitals are strongly stabilized owing to the excess of positive charge of the system.

We will discuss our results in the framework of the perturbation theory of reactivity. If only the denominator of the charge-transfer term of the interaction energy between the reactants is considered (third term in the Klopman-Salem<sup>35</sup> equation), the energy gaps in Figure 3 allow us to analyze which are the orbitals that could govern the regioselectivity of the nucleophilic aromatic photo-substitutions.

If the reaction takes place through the  $S_1$  state, the expected dominant interaction would be between the H orbital of the amine and the H orbital of the  $S_1$  of the aromatic substrate. Likewise, when the reaction proceeds via the  $T_1$  state, the most favorable interaction is assumed to be between the H orbital of the amine and the H  $\beta$ -spin orbital of the  $T_1$  state of the aromatic substrate. In both cases the relevant orbital in the excited aromatic substrate correlates with the HOMO of the ground state of 4-nitrophenol. This result is in good agreement with the predicted HOMO-controlled mechanism when the reaction involves a direct interaction between an excited aromatic substrate and a nucleophile.<sup>19-21</sup> However, the energetic order of the frontier orbitals found in the present work does not coincide with the proposed one by Mutai et al.<sup>20</sup> According to our results, the H orbital of the amines lies below both the H orbital of  $S_1$  and the H  $\beta$ -spin orbital of  $T_1$ . As a matter of fact, only this energetic arrangement of the frontier orbitals is able to produce a stabilizing interaction arising from the charge-transfer term, as a direct consequence of the algebraic form of the denominator of this term.<sup>35</sup> In other words, only when the energy of the interacting occupied orbital is lower than the energy of the interacting unoccupied orbital does the denominator become negative, producing a stabilization of the system.

On the other hand, if the nucleophilic photosubstitutions involve electron transfer from the amine to the aromatic substrate, it is not evident which pair of spin orbitals interacts predominantly. This is a direct consequence of the destabilization and stabilization of the 4-nitrophenol and amine spin orbitals, respectively, when the electron transfer occurs. This alters dramatically the ground-state orbital arrangement. As a matter of fact, the interaction between the occupied L  $\alpha$ -spin orbital of the RA of 4-nitrophenol and the unoccupied H  $\alpha$ -spin orbital of the amine radical cation would be destabilizing overall, and the alternative interaction between the unoccupied L  $\beta$ -spin orbital of the RA of 4-nitrophenol and the occupied H  $\beta$ -spin orbital of the amine radical cation would be irrelevant because of the large energy difference. Those two interactions would correspond to the predicted<sup>20,21</sup> LUMO control in these reactions.

Therefore, we consider that only the  $S_N2Ar^*$  reactions can be classified as frontier orbital controlled and, in particular, HOMO controlled. In Figure 4 the coefficients of the H orbitals for  $S_0$ ,  $S_1$ , and  $T_1$  electronic states of 4-nitrophenol are shown. Although these three orbitals correlate with each other, notice that the H orbital of  $S_0$  is a doubly occupied HOMO, the H orbital of  $S_1$  is a half-occupied orbital, while the H orbital of  $T_1$  is an empty  $\beta$ -spin orbital. The values of the coefficients vary as the electronic states change, but the main trends are kept. In particular, the largest coefficient always corresponds to the carbon atom that bears the nitro group. In this way the substitution of the nitro group of 4-nitroanisole is predicted

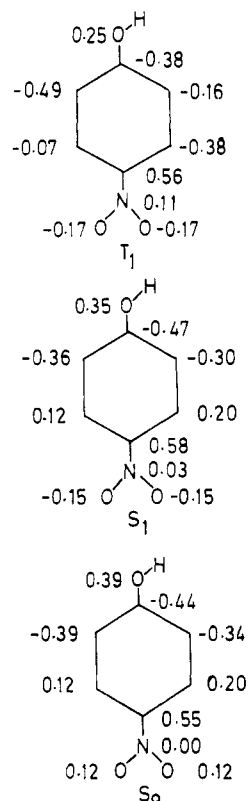


Figure 4. Coefficients of the H orbitals for  $S_0$ ,  $S_1$ , and  $T_1$  electronic states of 4-nitrophenol.

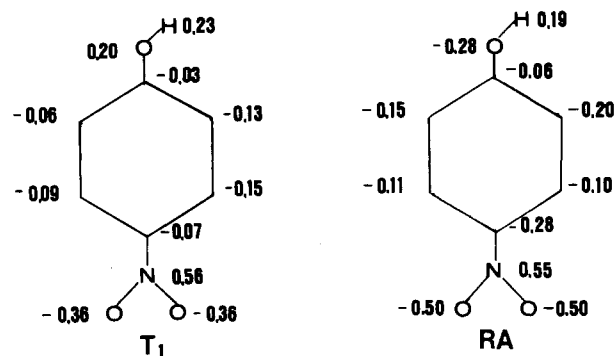


Figure 5. Net charges for the  $T_1$  excited state, and the RA of 4-nitrophenol.

in an  $S_N2Ar^*$  mechanism. In fact, this is the experimental behavior when ethyl glycinate is the nucleophile and 4-nitroanisole the substrate.

Different regioselectivity is found with *n*-hexylamine. As mentioned above, because of its lower ionization potential, *n*-hexylamine is able to react via electron transfer and subsequent recombination of the resulting radical ions. In this case, and considering the involvement of charged species, it seems logical to expect a charge-controlled mechanism (reactivity dominated by the second term of the Klopman-Salem<sup>35</sup> equation). In Figure 5 the net charges, based on a Mulliken's analysis, in the  $T_1$  of 4-nitrophenol and its radical anion are shown. First of all it should be remarked that for the  $T_1$  state both carbon atoms that bear leaving groups present similar net charges. The charges therefore do not appear to be important in determining the regioselectivity in  $S_N2Ar^*$  processes of 4-nitrophenol and 4-nitroanisole. Regarding the radical anion, the attack of a positive radical cation under charge control should take place at the most negative carbon atom of the aromatic ring, which in this case is that bonded to the nitro group. Therefore, the substitution of the nitro

(35) Fleming, I. *Frontier Orbitals and Organic Chemical Reactions*; Wiley-Interscience: New York, 1976; p 27.

group by attack of *n*-hexylamine should be also observed in this case. However, the photoreaction between 4-nitroanisole and *n*-hexylamine experimentally leads to displacement of the methoxy group. From our calculations we conclude that neither the frontier orbital nor the net charge seems to be the clue to explain the regioselectivity, in the 4-nitroanisole case, when the reaction involves electron transfer.

Among other possible factors, an important one, but not previously considered, is the relative stability of the two possible intermediate  $\sigma$ -complexes. The substitution of the nitro group is only observed when the C-N bond formation occurs in a "true" photochemical step ( $S_N2Ar^*$  mechanism, direct attack of the nucleophile on the substrate excited state), and no leaving group is present at the meta position with respect to the nitro group. In this case relatively low barriers are involved ( $k_3 > 10^8 \text{ M}^{-1} \text{ s}^{-1}$  in the preceding kinetic discussion), and the process will show a reactant-like transition state. This is the ideal situation for the use of the perturbation theory of reactivity in the interpretation of experimental results, and we have just shown this theory can justify the regioselectivity change between ground-state (LUMO controlled) and excited-state (HOMO controlled) nucleophilic aromatic substitution of nitrophenyl ethers when the process is a true  $S_N2Ar^*$  process. Using a complementary approach, Havinga et al.<sup>5</sup> have emphasized that for  $S_N2Ar^*$  reactions the preferred transition state leads to the least stable  $\sigma$ -complex (corresponding to the  $\text{NO}_2$  substitution in our case), in agreement with our results. On the other hand, the radical-ion pair collapse involved in the electron-transfer mechanism, although fast, is probably a thermal step, with a higher barrier than in the  $S_N2Ar^*$  case and less reactant-like transition state. The relative stabilities of the intermediate  $\sigma$ -complexes will be reflected in the relative stabilities of the respective transition states in this case justifying the no substitution of the nitro group when this mechanism operates.

### Experimental Section

**General.** All melting points are uncorrected,  $^1\text{H}$  NMR and  $^{13}\text{C}$  NMR spectra were recorded at 80 and 20 MHz on a Bruker WP80SY spectrometer using TMS as internal standard. IR spectra were recorded on a Perkin-Elmer 1310 spectrophotometer. UV spectra were recorded on a Hewlett-Packard 8452A diode array spectrophotometer. Mass spectra were recorded on a Hewlett-Packard 5985B mass spectrometer. The GC analyses were performed on a HP-5890A gas chromatograph using a HP-cross-linked dimethylsilicone gum 12 m  $\times$  0.2 mm  $\times$  0.33 m film thickness capillary column. Quantum yield measurements were performed on a Applied Photophysics QYR15 merry-go-round apparatus. The wavelength of excitation was selected using a Jobin Ivon monochromator.

***N*-(1-Hexyl)-4-nitroaniline (1).** Irradiation of a solution of 4-nitroanisole (0.88 g, 5.78 mmol) and *n*-hexylamine (15.25 g, 0.151 mol) in a mixture of 100 mL of methanol and 500 mL of water for 2 h in a Pyrex immersion well reactor using a 400-W medium-pressure Hg lamp as light source afforded starting material (4-nitroanisole, 0.343 g) and 0.128 g of product 1 (16% yield based in the consumed starting material), mp 61–63 °C, isolated by column chromatography through acid alumina using hexane as a eluent: IR ( $\text{CHCl}_3$ ) 3390, 1600, 1510, 1340, 1330  $\text{cm}^{-1}$ ;  $^1\text{H}$  NMR ( $\text{CDCl}_3$ )  $\delta$  0.9 (t,  $J = 5.1$  Hz, 3 H), 1.2–1.8 (m, 8 H), 3.2 (t,  $J =$

7.1 Hz, 2 H), 6.5 (d,  $J = 10$  Hz, 2 H), 8.1 (d,  $J = 10$  Hz, 2 H);  $^{13}\text{C}$  NMR ( $\text{CDCl}_3$ )  $\delta$  13.7, 22.3, 26.4, 28.8, 31.2, 43.2, 110.7, 126.1, 137.3, 153.6; MS,  $m/e$  (relative intensity) 222 ( $M^+ 12$ ), 151 (100), 105 (44), 76 (21), 55 (18), 43 (46), 41 (38). Anal. Calcd for  $\text{C}_{12}\text{H}_{18}\text{N}_2\text{O}_2$ : C, 64.84; H, 8.16; N, 12.60. Found: C, 64.98; H, 8.31; N, 12.71. Product 1 was also prepared in 18% yield (0.264 g) by heating at 180 °C, in a pressure-resistant reactor, 4-nitroanisole (1.023 g, 6.7 mmol) and *n*-hexylamine (7.62 g, 75.7 mmol) in methanol (110 mL) during 115 h under magnetic stirring.

***N*-Ethoxycarbonylmethyl-4-methoxyaniline (2).** Irradiation of 4-nitroanisole (0.723 g, 4.7 mmol), ethyl glycinate hydrochloride (5.619 g, 40.3 mmol), and sodium hydroxide (1.595 g, 40 mmol) in a mixture of 100 mL of methanol and 100 mL of water for 13 h, in the same general conditions used for the preparation of 1, afforded 0.124 g of product 2 (15% yield based in the consumed starting material; 0.032 g of 4-nitroanisole was recovered), mp 56–58 °C (lit.<sup>36</sup> 57–58 °C). Product 2 was also prepared in 31% yield (0.642 g) by refluxing 4-methoxyaniline (1.232 g, 10 mmol), anhydrous sodium acetate (0.82 g, 10 mmol), and ethyl chloroacetate (1.35 g, 11 mmol) in absolute ethanol (12 mL) for 14 h.

**Qualitative Experiments and Semipreparative Reactions (Table I).** Reaction mixtures were irradiated using a 125-W high-pressure Hg lamp as a light source. To ensure that different additives were not absorbing, a filter prepared with triacetic acid lactone (0.1 M) in *tert*-butyl alcohol ( $\lambda > 340$  nm) was used. The values in Table I correspond to the ratio between the chromatographic (GC) peak areas of the studied photoproduct in each case (identified by comparison with authentic samples prepared independently by thermal reactions), referred to the chromatographic peak area of a fixed amount of internal reference (4-nitroveratrole in the *n*-hexylamine cases and naphthalene in the ethyl glycinate cases) and the same in a blank experiment in the absence of additives. The used conditions and concentrations are given in Table I. The given values result from five independent measurements, eliminating the higher and lower ones and averaging the remaining three values.

**Quantum Yield Measurements (Tables II–V).** Quantum yields for the photoproducts were measured using a merry-go-round apparatus. The irradiation source was a 250-W medium-pressure Hg lamp. The wavelength of excitation (366 nm) was selected using a monochromator. Product appearance was monitored, and the amount of photosubstitution product (identified by comparison with authentic samples prepared independently by thermal reactions) in each case was determined by GC analysis (internal reference 4-nitroveratrole in the *n*-hexylamine cases and naphthalene in the ethyl glycinate cases). Actinometry was performed using potassium ferrioxalate,<sup>37</sup> and conversion was kept around 5% in all the cases. Care was taken that >98% of the light was absorbed by the sample and the actinometer. The temperature was kept at  $28 \pm 1$  °C in all cases. The concentrations of reactants are given in the tables. No precautions were taken with the presence of oxygen. All the values are the result of five measurements, eliminating the two extremes and averaging the other three.

**Acknowledgment.** Financial support from DGICYT ("Ministerio de Educación y Ciencia" of Spain) through Project No. PB87-0032 is gratefully acknowledged.

**Registry No.** 1, 84292-06-8; 2, 50845-77-7; *p*- $\text{O}_2\text{NC}_6\text{H}_4\text{OMe}$ , 111-26-2;  $\text{H}_2\text{NCH}_2\text{CO}_2\text{Et}\cdot\text{HCl}$ , 623-33-6.

(36) Kondo, K.; Hayazaki, T. *Yakugaku Zasshi*, 1961, 81, 97; *Chem. Abstr.* 1961, 55, 13350d.

(37) Calvert, J. G.; Pitts, J. N. In *Photochemistry*; Wiley: New York, 1966; p 784.